Hydrophobization of Silica Nanoparticles in Water: Nanostructure and Response to Drying Stress

Solenn Moro, Caroline Parneix, Bernard Cabane, Nicolas Sanson, Jean-Baptiste d'Espinose de Lacaillerie

Hydrophobization of Silica Nanoparticles in Water: Nanostructure and Response to Drying Stress

Solenn Moro,[†,‡,§] Caroline Parneix,[§] Bernard Cabane,[†] Nicolas Sanson,[†,‡] and Jean-Baptiste d'Espinose de Lacaillerie*[†]*

[†] PSL Research University, ESPCI Paris, CNRS UMR 7615 and UMR 8231, 10 rue Vauquelin, F-75231 Paris cedex 05, France

[‡] Sorbonne-Universités, UPMC Univ Paris 06, SIMM, 10 rue Vauquelin, F-75231 Paris cedex 05, France

[§] Saint-Gobain Recherche, 39 quai Lucien Lefranc, 93303 Aubervilliers Cedex

ABSTRACT

In this paper, we investigated the impact of surface hydrophobization on the structure of aqueous silica dispersions and how this structure resists drying stress. To achieve this, hydrophilic silica particles were hydrophobized directly in water using a range of organosilane precursors, with a precise control of the grafting density. The resulting nanostructure was precisely analyzed by a combination of small angle X-ray scattering (SAXS) and cryo-microscopy (cryo-TEM). Then, the dispersion was progressively concentrated by drying and the evolution of the nanostructures as a function of the grafting density was followed by SAXS. At the fundamental level, because the hydrophobic character of the silica surfaces could be varied continuously through a precise control of the grafting density, we were able to observe how the hydrophobic interactions change particles interactions and aggregates structures. Practically, this opened a new route to tailor the final structure, the residual porosity and the damp-proof properties of the fully dried silica. For example, regardless of the nature of the hydrophobic precursor, a grafting density of 1 grafter per nm^2 optimized the interparticle interactions in solution in view to maximize the residual porosity in the dried material (0.9 cm^3/g) and reduced the water uptake to less than 4 % in weight compared to the typical value of 13 % for hydrophilic particles (at T=25 °C and relative humidity RH=80 %).

1. INTRODUCTION

When an aqueous colloidal dispersion is dried, the concentration of the particles results in a stress build-up. Depending on the interaction potential between the particles, this added stress can result in various transitions through the colloidal phase diagram leading for examples to ordered solid states or to the formation of aggregated structures. The control of these phenomena is essential in many applications involving coating and drying. It is generally achieved by modulating the strength and the

range of attractive and repulsive interactions between nanoparticles. Silica particles constitute a convenient model system for the investigation of such phenomena because their surface chemistry in aqueous media is well known and make them good candidates for the study of aggregation processes. Indeed, variations of pH result in a modulation of the number of negatively charged silanolate surface groups while the range of the resulting repulsive electrostatic interactions can be controlled through the ionic strength of the suspending solution.[1, 2] Furthermore, aggregation of silica particles in aqueous solution can also be induced using multivalent ions[3] or polymers[4-7] leading to the formation of aggregates in aqueous solution.

Hydrophobic interactions can also modify the colloidal state of silica particles in water. However, those short-range attractive forces are not as commonly used as the one described above to induce the destabilization of silica particles in polar media. Generally, the main method reported in the literature to modify a particle's hydrophilic-lipophilic balance is through the adsorption of amphiphilic molecules, such as cationic surfactants or charged copolymers, whose hydrophilic part adsorbs onto the silica surface and whose hydrophobic part points outwards. In these systems, a fast flocculation occurs at low surfactant concentrations due to strong hydrophobic interactions between the modified silica particles.[8, 9] However, the amphiphilic molecules can easily be desorbed upon modification of the surrounding media and thus the silica hydrophobization can be reversible. When an irreversible hydrophobization is desired, hydrophobic species must be covalently grafted onto silica surface. This hydrophobic grafting of silica nanoparticles is performed through an hydrolysis-condensation mechanism of alkylsilanes with the surface silanol groups. The reaction is generally carried out in organic solvents[10-12] to insure that hydrolysis only occurs with the residual adsorbed water on the silica surface and that the condensation is principally obtained between the precursor and the silica surface.[10, 13] In this manner, a rather well-defined monolayer coverage of the silica surface can be obtained but this is at the inconvenience and cost of using an organic apolar solvent which must be further exchanged with water. Thus, during the last 20 years, numerous investigations were conducted on the hydrophobic

grafting in water-rich or biphasic media. De Monredon-Serani *et al.* studied the grafting of precipitated silica particles in a water / ethanol (25/75 v/v) mixture by alkylalcoxysilanes.[14] Schewertfeger *et al.* found that the hydrophobization of a xerogel with trimethylchlorosilane in water is possible by addition of hexamethyldisiloxane.[15] The principal inconvenient of such water-rich mixtures is the fact that the precursor must be introduced in large excess with regards to the reactive silanol functions on the silica surface. More recently, silica particles were chemically modified with high reaction yields thanks to multifunctional glycidoxysilanes or polyalkyleneoxysilanes in pure water.[16, 17] A good grafting efficiency was achieved with the dropwise precursor addition in the silica dispersion so that it preferentially reacts with the surface silica instead of inducing a self-condensation. Inspiring ourselves from this work, we have developed a protocol for the chemical modification of silica particles with pure hydrophobic silanes directly in water. This original chemistry provided an opportunity to study in water, without solvent exchange, the phase diagram of silica dispersions with respect to their hydrophobic character and applied drying stress.

In the present work, we investigate the relation between the chemical hydrophobization of silica nanoparticles in water and the resulting dispersion nanostructure, its drying behavior and the water uptake of the hydrophobized silica particles. To achieve this, hydrophilic silica nanoparticles were first hydrophobized in water using different hydrophobic organosilane precursors. The colloidal state of the modified silica dispersions was studied as a function of both the organosilane precursor's nature and the grafting density. Then, the resulting nanostructures were followed using cryo-transmission electronic microscopy (cryo-TEM) and small angle X-ray scattering (SAXS). As the drying state constitutes the ultimate concentration process in which capillary pressures are known to collapse porous structures, the impact of the silica hydrophobization in pure water on the structural changes upon drying has been investigated by SAXS experiments. In parallel, mercury intrusion porosimetry on dried powders gave complementary results on the aggregate's organization at larger scale upon drying in the final porous material. Finally, the damp-proof behavior of such hydrophobized silica particles was evaluated by

means of contact angle measurements on dip-coated colloidal films and water-uptake on the formed materials after drying. This set of analysis allowed us to respond efficiently to several questions:

(i) What is the impact of hydrophobization on the colloidal stability of the silica dispersion and consequently on their resulting nanostructure? Indeed, the presence of hydrophobic groups on the surfaces of neighbouring particles should change their interactions in solution.

(ii) Compared to pure hydrophilic silica particles where dense structures are obtained under drying, how do the structural pathways of hydrophobized silica evolve under drying stress? In other words, how does a hydrophobized silica dispersion dry?

(iii) Finally does this chemical hydrophobization induce damp-proof properties to the final material, that is to the dried modified silica dispersion? This can be appreciated through the water uptake of the silica material formed from the drying of the hydrophobized silica particles solution.

In short, by answering the questions listed above, we investigated in this paper the possibility and potential of ingeniously controlling in water nanoparticle interactions using hydrophobic grafters.

2. EXPERIMENTAL PART

2.1. Materials. A commercial Ludox® TM-50 colloidal silica, with a surface area of 140 m²/g, was used in this study. The average radius of the particles (R_p of 13 nm) and the width of the distribution ($\sigma R/R_p$=0.12) were determined by fitting the X-ray scattering curve of a highly diluted dispersion (volume fraction Φ_v = 0.005) with a Schultz distribution of homogeneous spheres (see **Figure S1** in Supporting information). The commercial dispersion was dialyzed (Spectra/por dialysis membrane MWCO: 12-14 kDa from SpectrumLaboratories, Inc.) against ultrapure water until its conductivity dropped below 150 μS/cm. The silica dispersion's pH was readjusted to 9.0 with a few drops of a concentrated (1 M) sodium hydroxide solution. Different methoxy hydrophobic organosilane precursors were used in the hydrophobization reaction: propyl(trimethoxy)silane (PTMS),

isobutyl(trimethoxy)silane (iBTMS) and dimethoxydimethylsilane (DDMS). All products (reagent grade) were purchased from Sigma Aldrich and used as received. Ultrapure deionized water with a minimum resistivity of 18 MΩ.cm (milliQ, Millipore, France) was used in the experiments.

2.2. Synthesis of Hydrophobized Silica Particles. After dialysis against ultrapure water, a 0.05 volume fraction aqueous silica dispersion at pH = 9.0 was stirred at 60 °C. Then, the methoxy hydrophobic organosilane precursor was very slowly added into the silica dispersion under vigorous stirring during 8 hours with a syringe pump and the mixture was kept at 60 °C under stirring during 24 hours. The amount of added organosilane precursors was varied to target a range of molar grafting ratio between 0 and 2 in order to reach different degrees of hydrophobicity. The molar grafting ratio is defined here as the ratio of organosilane precursors to the total surface SiOH groups assuming an hypothetical average surface density of 5 SiOH/nm^2.[18] Note that this target value thus correspond to a working parameter different from the actual grafting ratio which will depend on the grafting reaction efficiency and on the true silanol surface density. Finally, the silica dispersion was dialyzed against water at pH = 9.0 to remove the non-grafted precursors. At this stage, the volume fraction of silica in water was readjusted to 0.05. To assess the grafting efficiency, part of each sample, corresponding to about 1 g of modified silica was dried at 120 °C overnight and crushed with a pestle and mortar. The obtained powder was washed in a soxhlet device with a 1:1 dichloromethane / diethyl ether solvent to extract any adsorbed precursor left. Grafting efficiency measurements were performed on both the dialyzed modified silica and the particles washed with 1:1 dichloromethane / diethyl ether solvent. No significant difference was found between the two samples, indicating that dialysis is a sufficiently efficient purification step.

2.3. Concentration and Drying of the Silica Dispersions. 15 g of the silica dispersion, grafted or not, were introduced into different polypropylene containers with an internal diameter of 30 mm. The samples were let to concentrate and dry at 90 °C in an oven during 3 to 30 hours. Before analysis, the obtained concentrated pastes were re-homogenized by gentle manual stirring. The volume fraction, Φ_v, was determined by weighting dry extracts for each samples.

2.4. Characterization. *Thermogravimetric Analysis*. Thermogravimetric analysis (TGA) was performed using an SDT Q600 analyser from TA Instruments equipped with a flow gas system. After an isotherm at 110 °C during 20 min, the samples were heated up to 1150 °C with a heating rate of 10 °C/min in an air atmosphere. The weight loss of grafted silica can be attributed to (i) condensation of silanol groups (or dehydroxylation) and (ii) oxidation of the hydrophobic alkyl grafters (pretreatment at 110 °C for 20 min insured the prior removal of physisorbed water molecules). While dehydroxylation takes place over a large temperature range, the oxidation of the alkyl grafters takes place around 450 °C with only slight variations depending on the hydrophobic organosilane precursor. Finally, at 1150 °C, the dehydroxylation is complete and the silica surface is purely composed of siloxane bonds. The grafter's contribution and consequently the grafting density (number of grafters per nm²) was therefore obtained by subtracting the pure silica thermogram from the one of the modified samples and calculated by taking into account the alkyl chain's length. Moreover, TGA measurements allows us to directly derive a grafting surface density without assumptions on the silanol density and/or the chemical reactivity of the hydrophobic grafter. TGA measurements were repeated twice on several samples and found very reproducible, within 0.1 % of weight loss variation. The grafting density could therefore be determined when the TGA weight loss value was at least 0.3 wt % higher than the one for unmodified silica.

Microscopy. The colloidal dispersions were spread on ultrathin 300 mesh Formvar/carbon-coated copper grids and maintained in a frozen-hydrated state by quenching into liquid ethane cooled by liquid nitrogen. The cryofixed specimens were mounted into a Gatan cryoholder for direct observation at -180 °C in a JEOL 2100HC cryo-TEM operating at 200 kV with a LaB_6 filament. Images were recorded in zero-loss mode with a Gif Tridiem energy-filtered-CCD camera equipped with a 2k x 2k pixel-sized chip. Acquisition was accomplished with Digital Micrograph™ software.

Small Angle X-ray Scattering (SAXS). SAXS experiments were carried out on the SWING beamline at the Soleil Synchrotron (Saclay, France). The detector, an AVIEX CCD camera, was placed at 8 m from the sample. In this configuration, the *q*-range extended from 0.00107 to 0.152 $Å^{-1}$. All measurements

were done under atmospheric pressure, at 22 °C and in ambient humidity (relative humidity of 50 % measured with a humidity sensor). Diluted samples were studied in a fix capillary tube (diameter of 2.05 mm) whereas more concentrated dispersions were deposited in 1 mm gap hermetic cells with kapton films. The assembly was hermetically sealed to prevent drying. The backgrounds scattering from the empty and water filled measurement cells were subtracted from the intensity curves. More details on SAXS data processing are given in Supporting Information.

Mercury Intrusion Porosimetry. Mercury intrusion porosimetry measurements were performed with Pascal 140 and Pascal 240 porosimeters. The preliminary dried materials were maintained at 105 °C until the beginning of the measurement to prevent any re-adsorption of water. Approximately 0.2 g of sample was introduced into the measurement cell where a vacuum of 10 Pa was reached. The cell was filled with mercury and an increased pressure was applied on the cell up to a maximum of 200 MPa. The pore size's distribution was obtained assuming cylindrical pores.

Near Infrared Spectroscopy. The near infra-red spectra were recorded using a Bruker NIR-MPA at ambient temperature and humidity.

Contact Angle Measurements. Contact angle measurements were carried out on dip-coated silica dispersions. The thicknesses of the films were measured using a 3D optical profilometer (FOGALE nanotech). The thin films were maintained in a controlled relative humidity of 43 % thanks to a saturated aqueous solution of potassium carbonate K_2CO_3. A 3 µL drop of ultrapure deionized water was deposited on the surface and the drop's profile was recorded over time with a monochrome video camera. Contact angles were obtained from the drop's profiles.

Water Adsorption. Water adsorption measurements were realized on the modified silica. After a 48 h drying performed at 120 °C in an oven, the powders were introduced in an environmental test chamber Espec SH-641 at 25 °C and a relative humidity of 80 %. The powders weight increase was followed over time until equilibrium which can take from several days to several weeks depending on the hydrophilicity of the silica surface.

3. RESULTS AND DISCUSSION

3.1. Hydrophobization reaction. The hydrophobization of silica particles was performed in water by grafting hydrophobized organosilane precursors on SiOH groups located at the silica particle surfaces. The introduced molar grafting ratio was defined as the number of organosilane precursors divided by the total number of SiOH groups assuming an average surface density of 5 SiOH/nm^2.[18] The hydrophobized precursors were very slowly added to the silica dispersion in order to favor their grafting on silica surface whilst avoiding their reaction with each other (self-condensation) in water. Methoxy-organosilane precursors were preferred from halogenated precursors in order to avoid the formation of hydrochloric acid that modifies both the pH and the ionic strength of the solution and consequently can change the colloidal stability of the silica dispersion. Depending on both the molar grafting ratio and on the organosilane precursor, the silica dispersions went from slightly turbid to completely opaque and viscous for high grafting ratios (see **Figure S2** in Supporting Information). The efficiency of the hydrophobization reaction was evaluated through thermogravimetric analysis (TGA) by measuring the evolution of the experimental grafting density as a function of the amount of grafters introduced in the systems for different hydrophobic organosilane precursors (see experimental part). The results are shown in **Figure 1**. At low grafting densities, for PTMS and iBTMS grafters, it appeared that the grafting densities were roughly linear with the amount of introduced grafters, regardless to the alkyl chain's length and reached an efficiency of 20-30 % on average. In this range, the hydrophobization caused little changes of turbidity (see **Figure S2** in Supporting information). Note that for the DDMS precursor, the TGA was insufficiently sensitive, as the weight loss was too small to provide accurate values for low grafting densities. For higher grafting densities and for all the studied precursors, the grafting efficiencies were not constant and increased to about 56 %. The boundary between high and low grafting densities matched to the point where the solution exhibited a significant macroscopic visual

aspect change from translucent to very turbid samples (see **Figure S2** in Supporting information). It could thus be assumed that, in our experimental conditions, at low grafting ratios, the precursor condensation preferentially took place with the surface silanol groups. On the contrary, at higher ratios, the self-condensation dominated leading to an efficiency of 100 % as shown in **Figure 1**. Such efficiency is possible only if one considers that for this amount of introduced grafters, all introduced organosilane precursors reacted with each other in solution.

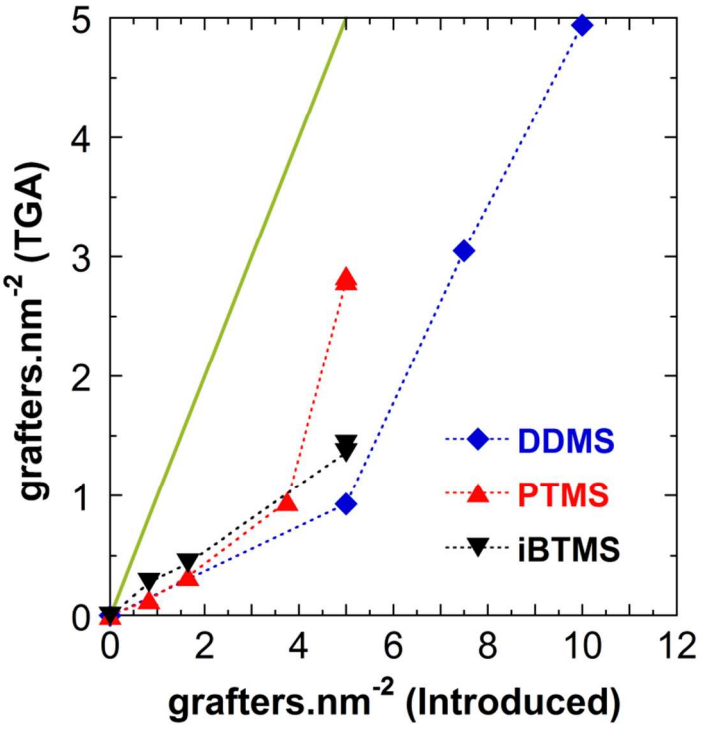

Figure 1. Grafting efficiency evaluated by TGA for dimethoxydimethylsilane DDMS (◆), trimethoxy(propyl)silane PTMS (▲), isobutyl(trimethoxy)silane iBTMS (▼). The solid line (green) represents a theoretical 100 % grafting efficiency.

3.2. Nanostructure in Solution. In order to investigate the influence of the hydrophobization reaction on the colloidal state of the silica nanoparticles in aqueous solution, we performed a coupled cryo-TEM / SAXS study on silica particles that had been hydrophobized with the dimethoxydimethylsilane precursor (DDMS). The results are presented in **Figures 2 and 3**. **Figure 2** shows cryo-TEM images of

hydrophobized silica solutions at different grafting densities with dimethyldimethoxysilane (DDMS) as organosilane precursor. SAXS measurements were performed on the same samples (0.05 volume fraction) and the scattered intensity profiles of those modified silica dispersions were represented in **Figure 3**. The scattering profile of non-grafted hydrophilic silica dispersion at high pH (pH = 9.0) and low ionic strength shows a strong depression at low q values followed by a scattering peak at q_{peak} = 0.011 $Å^{-1}$ matching approximately an average interparticle distance at this concentration $d = 2\pi/q_{peak}$ of 55 nm. This profile is characteristic of a concentrated dispersion of repelling particles. Indeed it can be well fitted using the Mean Spherical Approximation (MSA) which takes into account the repulsive interactions between charged colloids (see **Figure S3** in Supporting information).[19] At low q values, i.e., for values corresponding to distances higher than the mean interparticular distance, the scattered profiles exhibit a plateau which indicates that the system is homogeneous at these scales. The interparticle center-to-center distance determined from the peak position (d = 55 nm) is consistent with the average distance measured between the particles on cryo-TEM image (d = 52 ± 5 nm) (see **Figure 2a**).

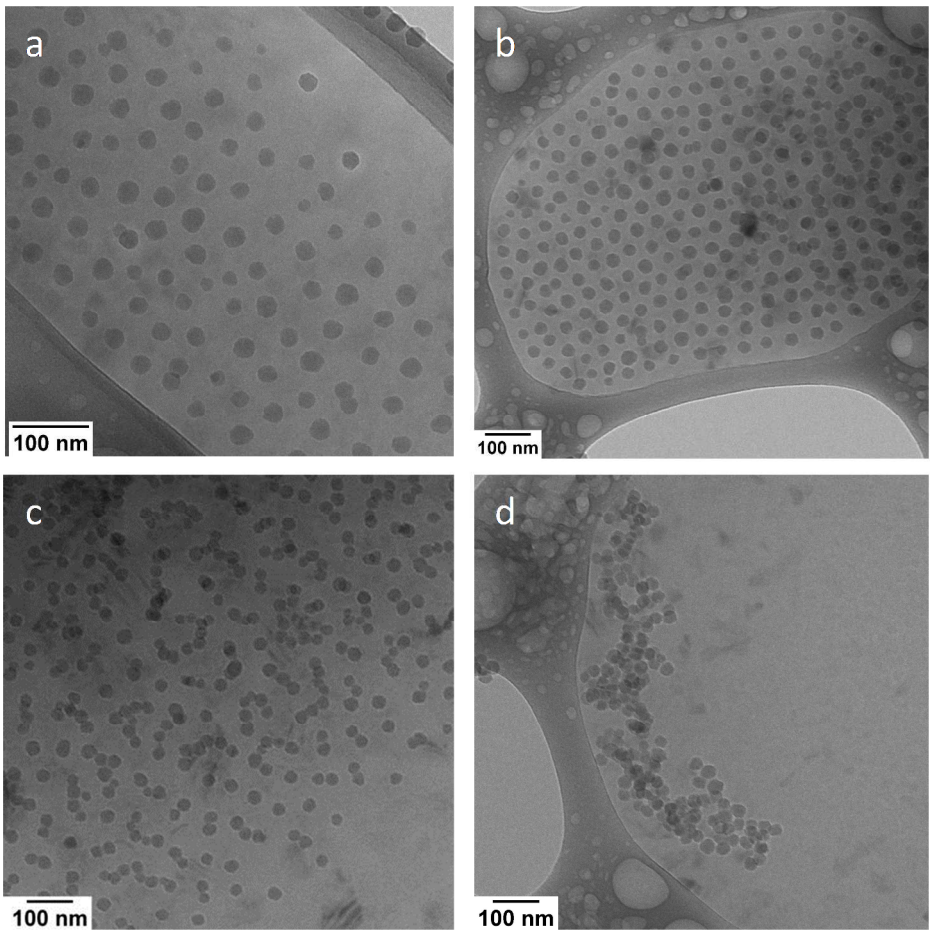

Figure 2. Cryo-TEM images of modified silica dispersions with dimethoxydimethylsilane (DDMS) at different grafting ratios: (a) hydrophilic silica dispersion, (b) 0.7 grafters per nm², (c) 0.9 grafters per nm² and (d) 3.0 grafters per nm². For sample (b), due to the TGA detection limit, the exact grafter density is not known. The value of 0.7 grafters per nm² is assumed from the introduced amount taking the grafting efficiency of the 0.9 grafters per nm² sample, i.e. 18 %. (see Figure 1).

Under the same conditions, the slightly hydrophobized silica particles, i.e., with a low grafting density (0.7 grafters per nm²), remained also well dispersed in water as observed on the corresponding cryo-TEM image (**Figure 2b**) where a similar organization was evidenced. Its scattered intensity profile slightly changes over the whole *q* range compared to the scattering profile of a dispersion of hydrophilic silica particles in similar conditions of pH and ionic strength (see **Figure S4** in Supporting information). Consequently, a surface modification of 0.7 grafters per nm² produced no measurable differences in the organization of the particles in the dispersion.

By increasing the grafting density to 0.9 grafters per nm², the SAXS profile and the colloidal organization in the cryo-TEM image were modified. On the one hand, as the grafting density increases, the position of the structural peak shifted from 0.011 $Å^{-1}$ in the case of pure hydrophilic silica particles to 0.0092 $Å^{-1}$ for hydrophobized silica particles indicating a higher average distance (d = 68 nm) between the particles. Also remarkable was the fact that the height of the constant intensity plateau at q values lower than 0.005 $Å^{-1}$ was increased for this modified silica dispersion with regards to the purely hydrophilic dispersion. Accordingly, the spatial distribution of the particles was less homogeneous than in the two previous cases: this was also in line with the observed increase of the structural peak width. Since the scattering profiles I(q) were similar at high q values, corresponding to intraparticle distances, the increase of the intensity at low q values($q < 0.005$ $Å^{-1}$) means that the hydrophobization reaction has perturbed the interparticle correlations, leading to a less organized system. This is characterized by a pair correlation g(r) or by its Fourier transform, the structure factor, $S(q)$ with weaker oscillations (see Supporting Information). This is also supported by the cryo-TEM observations showing a heterogeneous system in which smaller linear aggregates made of two to six silica particles coexisted with isolated silica particles (see **Figure 2c**). Note that the aggregation observed by both experiments can also be correlated with the observed turbidity increase (**Figure S2** in Supporting information).

Finally, at a even higher grafting density (3.0 grafters per nm²), a white and viscous suspension was obtained (**Figure S2** in Supporting information) and larger objects, extending over several hundreds of nanometers, were observed according to the cryo-TEM image (**Figure 2d**). No residual isolated silica particles were detected. The formed aggregates were not fully dense and an intra-aggregate porosity appeared in the electronic microscopy observations. The SAXS profile for the same silica particles hydrophobized with a grafting density of 3.0 grafters per nm^2 corresponds to an aggregated system exhibiting an intensity increasing at low q values where I(q) varies as q^{-2} over more than one decade. We can also notice that no structural peak was observed for the aggregated system in the q region lower than 0.025 $Å^{-1}$. This means that the number of neighbors constituting the coordination shell of one silica particle was low, thus indicating the formation of loose aggregates. The value of the exponent of the

scaling law is close to what is expected from a reaction limited cluster aggregation (RLCA) process.[20, 21] Together with the absence of a structure peak, this might be taken as a manifestation of aggregation in presence of long-range electrostatic repulsions preventing formation of dense aggregates.[22]

As for the other studied hydrophobic precursors (PTMS and iBTMS), similar trends in terms of scattering profiles and colloidal state were observed with the increase of the molar grafting ratio. **Table S1** resumes the aggregation state, determined by cryo-TEM observations (see **Figure S5** in Supporting information), of the samples obtained with the range of hydrophobic organosilane precursors used in this study at various grafting densities. In all cases, modified silica nanoparticles remain isolated at low grafting density and then progressively aggregate in small linear aggregates followed by 3D-fractal aggregates for higher grafting density (**Figure 2**).

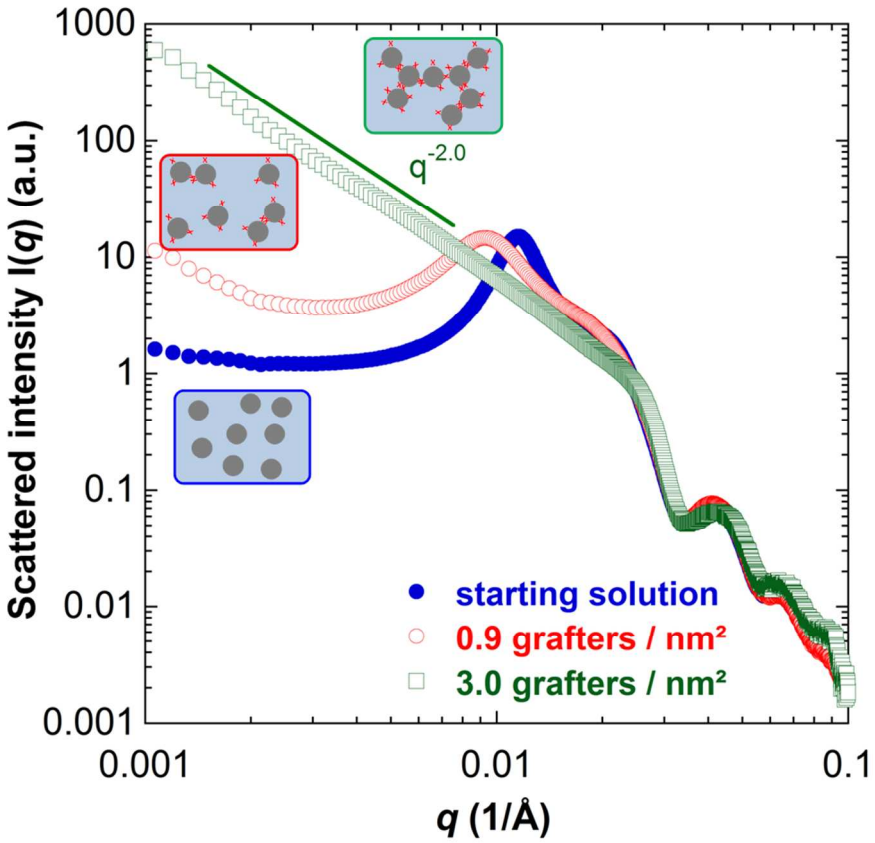

Figure 3. Scattered intensity I(q) of modified silica dispersions (Φ_v = 0.05) with dimethoxydimethylsilane (DDMS) at different grafting densities expressed as the number of grafters per nm^2 (●) hydrophilic silica particles, (○) 0.9 grafters per nm² and (□) 3.0 grafters per nm². All spectra were normalized at high q values. The inserts display schematically the corresponding colloidal states.

To summarize, the combined cryo-TEM / SAXS study revealed that the increase in grafting ratio was responsible for a controlled and progressive aggregation in water. For low grafting densities, the colloidal stability was maintained as the long range electrostatic repulsions overpowered the short range Van der Waals and hydrophobic interactions. At some point, between 0.7 and 0.9 grafters per nm^2, the strength and range of the hydrophobic increased and started to counteract the electrostatic repulsion. The hydrophobized particles aggregated into doublets and then, progressively, into small linear chains. The aggregate structures were determined by the balance between the hydrophobic interactions and the still present longer-range electrostatic repulsions that prevented the collapse of the aggregates in dense structures. This behavior is quite similar to what has already been observed in the case of silica aggregation in presence of polymers.[23, 24] Finally, 3D-aggregates with a fractal dimension of 2.0 were formed, probably because at the highest grafting ratios, the inter-polymerization of the precursors allowed a bridging between modified silica particles.

3.3. Resistance to Drying Stress. As mentioned above, the hydrophobization performed in water with hydrophobic organosilanes changed the way they interact with each other and also induced a progressive aggregation of the silica nanoparticles. This can be further probed by studying the response of the nanostructures to a compressive stress due to evaporation of the continuous water phase. Starting from a dispersion with a volume fraction $\Phi_v = 0.05$, water was progressively removed by evaporation at 90 °C (see experimental part). As the form factor of the silica particles does not evolve during the concentration process, we only focused on the evolution of the structure factor as a function of the silica volume fraction. **Figure 4** presents the resulting structure factor, $S(q)$, for the dispersion of pure hydrophilic silica nanoparticles, hydrophobized silica particles with dimethyldimethoxysilane (DDMS) at 0.9 grafters per nm² where small linear aggregates were present in solution and at 3.0 grafters per nm² where 3D-aggregates were present.

Hydrophilic silica. For the untreated hydrophilic silica particles dispersion ($\Phi_v = 0.05$, high pH and low ionic strength), the structure factors are typical of a repulsive system. As illustrated in **Figure 4a**, when increasing the silica particles volume fraction through evaporation of the liquid dispersion, the position of the main peak of $S(q)$ shifted to higher q (shorter distances) as the inverse cube root of the volume fraction, indicating that the particles come closer to each other as in a homogeneous compression (**Figure S6** in Supporting information). The increase of the main structure peak height (inset of **Figure 4a**) from a value S_{max} equal to 1.8 ($\Phi_v = 0.05$) to 3 ($\Phi_v = 0.26$) as well as the progressive decrease of the $S(q)$ plateau value at small q values ($0.001\ Å^{-1} < q < 0.01\ Å^{-1}$) down to a minimum value $S_{min} = 0.007$ also confirms that the spatial distribution of particles remained homogeneous upon concentration. The S_{max} values obtained during the first steps of concentration were consistent with those observed in colloidal systems exhibiting an ordered structure.[25, 26]

At high volume fraction in the liquid state ($\Phi_v = 0.26$), the main peak height reached $S_{max} = 3$. According to Verlet[27] and Hansen[28] when this degree of short-range order is reached, the liquid state with short-range order becomes unstable with respect to a state with long-range order (i.e. a colloidal crystal). However, the hydrophilic silica dispersion failed to crystallize, presumably because the time required for producing crystal nuclei was longer than the evaporation time. As a result it remained in a liquid like state where the particles were still separated by distances in the order of 9 nm. The same phenomenon took place in the sample that was dried to $\Phi_v = 0.6$, where the particles were only 1 nm apart, on average, and had lost all the mobility required for crystallization. The decrease in the height of the main peak of $S(q)$, from 3 to 1.9 (**Figure 4a**) and the increase in its width confirm that the dispersion was on its way to a colloidal glass state. All these observations on the structural changes observed during the drying of hydrophilic silica dispersions were consistent with the observation of Li et al. on the drying of dip-coated silica films.[29]

Finally, as shown in **Figure 4a**, the structure factor $S(q)$ for the final dry state presents a slow $q^{-1.8}$ decay at low q values. This departure from the q^{-2} scaling may reflects large scale defects in the

structure such as lumps, voids or cracks. In spite of those defects, the material tended towards a solid volume fraction of 0.65, very close to the close random packing of spheres ($\Phi_v = 0.64$).

Intermediate grafting regime. For a significant grafting of hydrophobic precursor on the silica surface (0.9 grafters per nm^2), the behavior of the hydrophobized silica upon concentration was significantly changed (**Figure 4b**). At the initial volume fraction, the position of the primary peak, its width as well as the slow decay at low q values reflected a more aggregated state compared to untreated silica, thus concurring with cryo-TEM observations (**Figure 2c**). As expected, the structure peak was shifted to higher q values upon increasing concentration because of the decrease of the average distance between particles upon concentration. However, contrary to non-modified silica, the structure peak height progressively decreased until its full disappearance. Hence, the initial dispersion state composed of isolated particles and small linear chains was not maintained during the concentration process of the system. Furthermore, a dramatic change of behavior occurred at $\Phi_v = 0.15$. Indeed, a strong low-q scattering replaced the broad depression that reflected the short-range order of repelling hydrophilic particles. This low-q scattering had a slow $q^{-1.3}$ decay. It was followed by a "hump" at the contact distance of the silica particles. This is consistent with the occurrence of the larger structures that increase the spatial inhomogeneity of the sample. This drastic change of the dispersion structure can have as origin an accretion of the original aggregates and particles when they are close enough to bind to each other through hydrophobic interactions. The absence of structure peak close to the characteristic distance of one elementary particle implies an incomplete coordination shell for each particle which is compatible with an open structure for the aggregates. The observed aggregation happens much sooner than with non-modified particles which were able to reach a density close to the one of random packing before being aggregated. As already stated, the slow decay at low q values means that lumps and voids were present at large scales. However, upon further concentration and drying, it can be expected that the structure collapses under capillary pressure and voids progressively suppressed. Indeed, when the volume fraction reached $\Phi_v = 0.31$, the depression in the structure factor curve deepened indicating a

decrease in the concentration fluctuations at smaller scales. In the final drying step, the steeper decay ($q^{-2.8}$) observed at very low q values indicates the presence of large aggregates in the final structure. It is noticeable that the structure factor minimum value in the depression for the dried state (S_{min} = 0.042) is more than 6 times higher than the one for the dried hydrophilic silica (S_{min} = 0.0068) meaning that even if, in both cases, the aggregated structure in the liquid state collapses under capillary forces, the amount of residual voids due to the defects in the final material are higher for hydrophobized silica particles.

Hydrophobic silica. Finally, contrary to the first two previous cases where a progressive decrease of the average interparticle distance was obtained upon concentration, the structure factor $S(q)$ for silica particles hydrophobized with the highest grafting density, i.e., 3.0 grafters per nm² (**Figure 4c**), exhibits a structure peak at an average interparticle distance of 22 nm which roughly corresponds to the particle's size. In plain terms, this means that particles were already in contact with a significant number of particles in the coordination shell of a given particle as also reflected in the significant height of the structure peak. On the other hand, at low q values (q < 0.01 Å^{-1}), the structure factor $S(q)$ followed a power-law in q^{-2} corresponding to an reaction-limited cluster aggregation. As we can see in **Figure 4c**, drying occurred in two steps. During the first step, from Φ_v = 0.05 to 0.23, the structure peak position remained unchanged whereas its height increased (from 1.3 to 1.9) which indicate that, at shorter distance, the number of neighboring particles at the same average distance increased. At longer distance (shorter q values), all the $S(q)$ curves superimposed meaning that the intra-aggregate structure was not affected by the sample concentration and that the inter-aggregate average distance was larger than what could be probed by our experimental range in q-range (up to 600 nm). In a second step, from Φ_v = 0.23 to the dry state, as the concentration increases further until the drying state, capillary forces induce a drastic collapsing of the porous structure where both the larger aggregates get closer and the voids are progressively suppressed as supported by the significant depression of $S(q)$ intensity around q = 0.01 Å^{-1}. It remains that the minimal value of the structure factor, S_{min} = 0.26, was 6 times higher than the one found at a grafting density of 0.9 and 38 times higher than the one found for non-modified silica particles. This revealed that silica hydrophobization led to a less dense structure associated to residual

intra-aggregate porosity. In our study, the compressive stress could not be measured but a comparison based on the minimum value of the structure factor can be made with results obtained by Madeline et *al.* which studied the restructuring of colloidal silica cakes under compression with pressures as high as 400 kPa.[30] In that situation, voids between aggregates are progressively compressed but a very steep decay (q^{-4}) at low q values is observed at high pressures. This q^{-4} power law is attributed to the formation of dense lumps between aggregates which build a skeleton rigid enough to prevent any further collapsing. In our case, during the ultimate drying step, the applied pressure is due to the Laplace forces and thus much higher than the 400 kPa applied in Madeline's work. Nevertheless, despite a more loosely connected skeleton, the porous structure resisted in similar ways. This similar resistance to collapse was established by the obtained decay rate of the structure factor which did not evolve with the drying step even when the silica dipersion was fully dried. Moreover, the minimal structure factor value S_{min} was in the same order of magnitude than the one obtained in the case of filtrated dispersions.[30] However, in our case, the slower decay rate q^{-2} instead of q^{-4} may be attributed to a stronger mechanical resistance of our aggregates, leading in our case to fractal lumps instead of a dense skeleton in a matrix of smaller density.

To summarize, from SAXS experiments, the main conclusions concerning the drying process of hydrophilic and hydrophobized silica particles was that (i) the drying of hydrophilic particles leads throughout the whole process to the progressive concentration of a homogeneous structure and therefore the formation of a dense network (ii) in contrast, the concentration of modified silica particles only results in the partial suppression of voids in the dried structure and the initial aggregated structures were thus maintained.

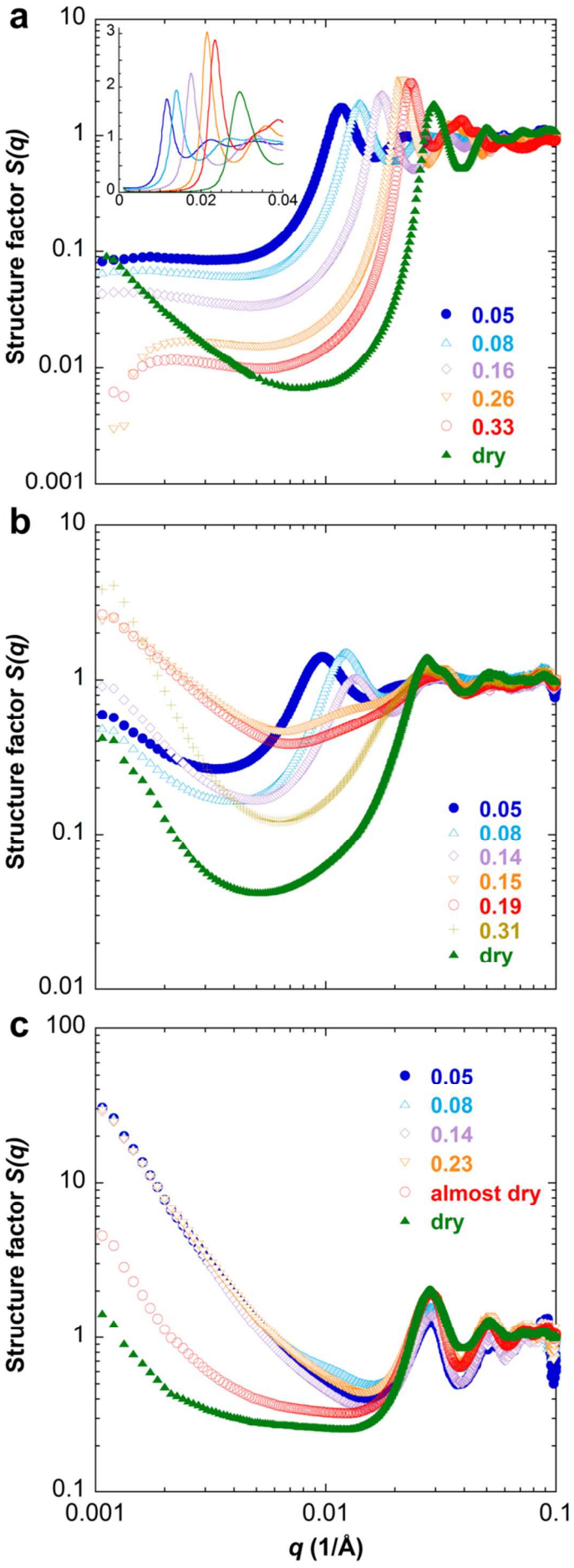
a
Structure factor S(q)
10
1
0.1
0.01
0.001
0.05
0.08
0.16
0.26
0.33
dry
b
Structure factor S(q)
10
1
0.1
0.01
0.05
0.08
0.14
0.15
0.19
0.31
dry
c
Structure factor S(q)
100
10
1
0.1
0.05
0.08
0.14
0.23
almost dry
dry
0.001
0.01
0.1
q (1/Å)

Figure 4. Structure factor $S(q)$ of silica dispersion at different concentration (volume fraction) obtained by drying (a) pure hydrophilic silica particles (the inset presents the structure factor in lin-lin scale in order to better visualize the evolution of the peak's height and width with the concentration and drying); (b) modified silica with dimethoxydimethylsilane (DDMS) at 0.9 grafters per nm²; (c) modified silica with dimethoxydimethylsilane (DDMS) at 3.0 grafters per nm².

3.4. Residual porosity in the dried state. As illustrated in **Figure 4**, the final structure made from hydrophobized silica particles diverges from the close random packing behavior of a repulsive and fully dispersed system observed in the case of hydrophilic particles. The residual porosity of the obtained powders after drying has been measured by mercury intrusion porosimetry analysis on modified and unmodified dried silica dispersions. The final porous volume as a function of the grafting density is represented in **Figure 5** for silica particles hydrophobized with different organosilane precursors. The typical evolution of the cumulative porous volume as a function of the pore radius as well as the pore size distribution for silica particles hydrophobized with dimethoxydimethylsilane (DDMS) are presented in **Figure S7** in Supporting information. As shown in **Figure 5**, it appears that, irrespective of both the functionality and the alkyl chain length of the organosilane grafter's, the residual porous volume gradually increased with the grafting density from 0.08 cm^3/g for powder made from pure hydrophilic silica particles until 0.85 cm^3/g for the highest grafting ratio in the case of DDMS. In addition, the pore radius is increasingly shifted towards higher values with the grafting ratio as illustrated in **Figure S7** in Supporting information. Cumulative porous volume as well as the range of pore radius for the different studied organosilane precursors were summarized in **Table S1** in Supporting information. For all grafters considered, the same trend of increasing porous volume and pore radius range was observed as a function of the grafting ratio.

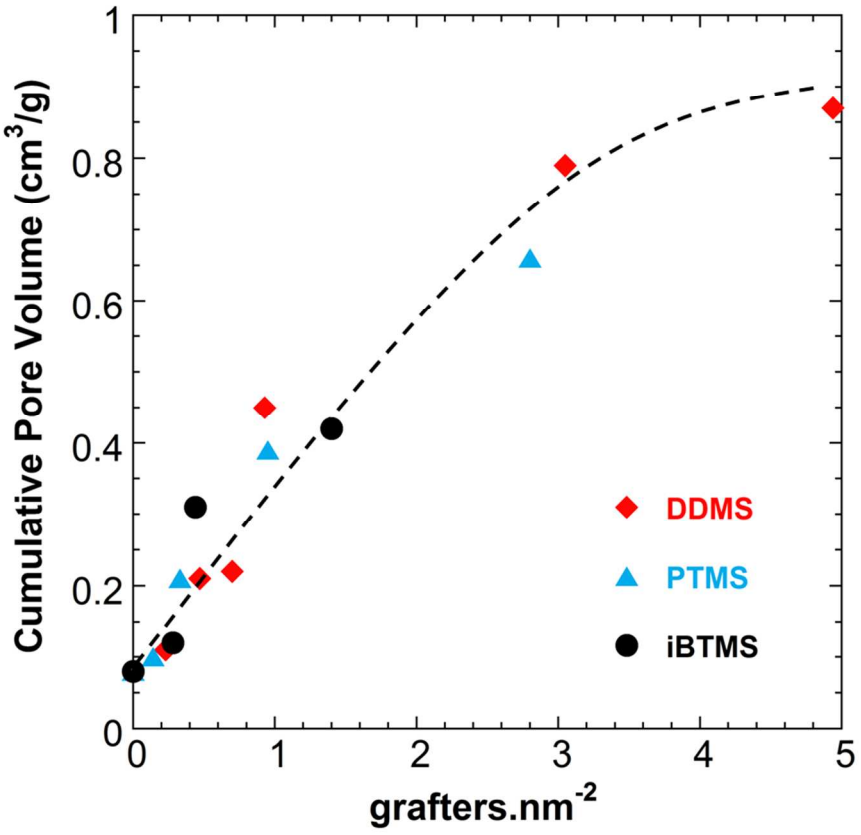

Figure 5. Porous volume of dried modified silica dispersions with the different studied precursors as a function of the grafting density: (◆) dimethoxydimethylsilane (DDMS), (▲) trimethoxy(propyl)silane (PTMS) and (▼) isobutyl(trimethoxy)silane (iBTMS). The dashed line is a guide for the eye. Concerning DDMS, the exact value of the grafters density for the first two points is not known due to the detection limit of the TGA method. For these points, values plotted are obtained by interpolation using the known introduced amount and assuming a grafting efficiency of 18 %.

Here, as shown in **Figure 5**, the drying of the unmodified hydrophilic silica particles at pH 9 and low ionic strength leads to a very low cumulative porous volume (0.08 cm^3/g) and a pore size distribution lower than 5 nm consistent with a well ordered dense system as observed in the case of silica colloidal crystals.[31] With increasing the grafting density, one observed a progressive rise in residual porosity after drying until 0.4 cm^3/g and a maximum pore radius of about 20 nm for a value of grating ratio about 0.9 grafters per nm^2. This reflected upon how surface hydrophobization modified the packing of the individual particles. Indeed, the introduction of an additional attractive component to the interaction potential between particles allowed the formation of small linear chains in addition to

individual particles (see cryo-TEM images in **Figure 2c**). A higher initial disorder at short-range caused eventually a more random, and so less dense, packing as supported by SAXS experiments (**Figure 4**) leading to a second-level of disorder in the structure. Then, the residual porosity obtained for low grafting densities would be the direct result of this disorder caused by the hydrophobization. In that case, the pore size was expected to remain low since it would scale mainly with the initial "structure defects", that are small linear chains. Indeed, pore size distributions (**Figure S7** in Supporting information) clearly showed very low pore radius values, comparable to the particle size at most. Finally, for higher grafting density which leads to an initial structure in solution made of large aggregates (**Figure 2d**), the cumulative porous volume increased to 0.8 - 0.9 cm^3/g and a maximum pore radius size of 40 nm was reached, commensurate to the voids size within the aggregates initially present in solution.

In the light of cryo-TEM, SAXS and porosimetry experiments, we can conclude that the dried samples exhibited a structure with three-levels of porosity. The first one is expected at a very low scale due to the random packing of the aggregates, similar to the one found for the dispersed silica particles. A second one, medium scale porosity, corresponded to the large voids in the aggregates' structure of approximately 50 nm in diameter. Finally, an even larger porosity, ranging up to 500 nm, remained after the imbrication of those very rough-shaped, full of cavities objects. The porosity remaining after drying correlated well with the grafting density irrespective of both the length and the nature of the hydrophobic grafters. However, as soon as inter-precursor condensation occurred leading to 3D-aggregates, further grafting agent addition had no significant impact neither on the nanostructure nor on the residual porosity after drying. As a consequence, the porous volume gain slows down after a density of 3 grafters per nm^2 to reach a maximum value of about 0.9 cm^3/g.

3.5. Hydrophobic properties of the dried silica. The hydrophobization of silica particles in water not only induces structural changes from the dispersed to the fully dried state, but also provides a progressive macroscopic damp-proof behavior. In order to investigate the influence of the performed

chemical modification on the wetting properties, contact angle measurements of a water drop were performed on colloidal thin films prepared by dip-coating a glass slide with modified and unmodified silica. For each sample, film thicknesses were varied from 150 to 600 nm and the measurements were performed 3 times for each film. The contact values were found very reproducible and independent of the film thickness. Note that the effect of hydrophobization was exclusively studied for low grafting densities where silica particles remained sufficiently well dispersed to allow the formation of homogeneous films. The resulting contact angles measurements as a function of the grafting ratio for different organosilane precursors are presented in **Figure 6** whereas both contact angle and radius drop kinetics for thin films constituted by silica particles modified by dimethoxydimethylsilane (DDMS) precursors, at different grafting ratios are shown in **Figure S8** in Supporting information. On the one hand, it clearly appears that, whatever the precursor's nature of the hydrophobic grafters, the apparent contact angle increased with the grafting density, from 3-4° for pure hydrophilic silica particle to a maximum value of 47° for hydrophobized silica with the highest grafting coverage. On the other hand, for slightly modified silica, when the drop was deposited on the film surface, its apparent contact angle rapidly decreased until reaching its equilibrium value after several seconds (see **Figure S8** in Supporting information). For instance, the apparent contact angle went from 6.6° to 3.8° after 12 s for pure hydrophilic silica films and this phenomenon was also observed for silica modified with DDMS with low grafting ratios. This decrease corresponds to the fast spreading that occurs onto the hydrophilic porous thin-film. However, this decrease at short time was totally suppressed for more hydrophobic silica (**Figure S9** in Supporting information).

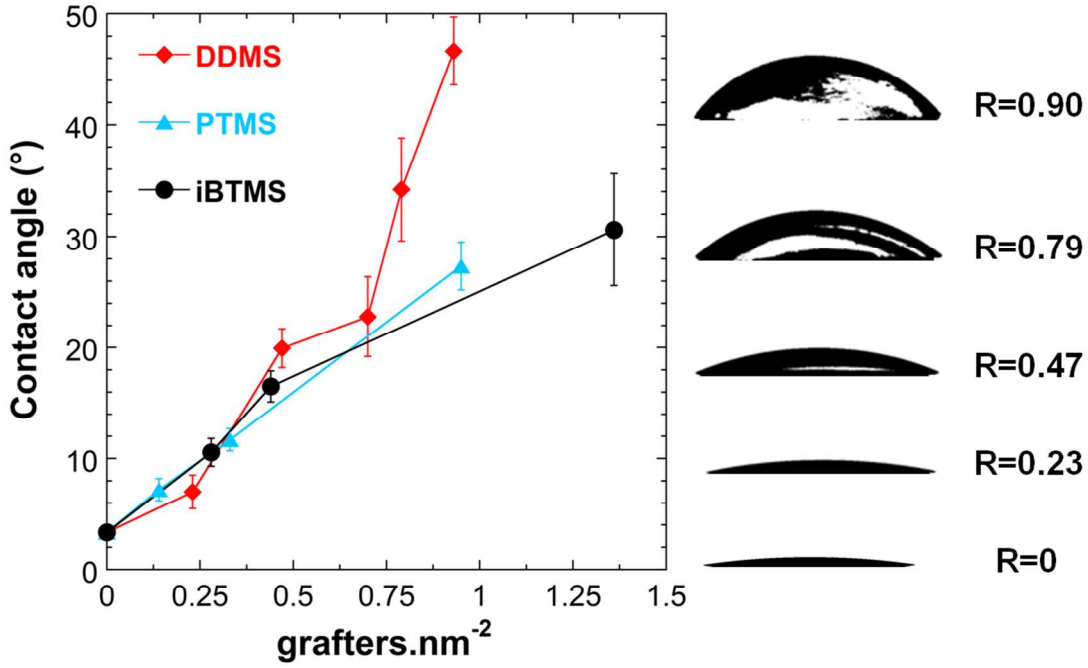

Figure 6. (left) Water contact angle values at 50 s as a function of the grafting density for dimethoxydimethylsilane DDMS (◆), trimethoxy(propyl)silane PTMS (▲) and isobutyl(trimethoxy)silane iBTMS (▼). (right) Images of water contact angle on silica hydrophobized with dimethoxydimethylsilane (DDMS) as the function of the grafting ratio. It was considered that after 50 s, the equilibrium state is reached (static contact angle) as shown the contact angle kinetics in Supporting information. Concerning DDMS, except for the first and last point, the exact value of the grafters density is not known due to the detection limit of the TGA method. For these points, values plotted are obtained by interpolation using the known introduced amount and assuming a grafting efficiency of 18 %.

Another direct consequence of silica hydrophobization is a modification of its ability to adsorb water. To examine this effect, the water uptake at 25 °C with a relative humidity of 80 % of a previously dried silica dispersion was studied. The **Figure 7a** presents the water uptake kinetics of dried silica particles hydrophobized with dimethoxydimethylsilane (DDMS) at different grafting ratios. As we can see, at short time, the water uptake rapidly increases to reach an equilibrium plateau. The value of the plateau depends on the molar grafting ratio; the higher the grafting ratio is, the lower the plateau value at the equilibrium time is. Similar trend was observed whatever the nature of the hydrophobic grafter. The weight increase at equilibrium as a function of both the grafting density and the organosilane precursor's

nature is reported in **Figure 7b**. As expected, unmodified silica particles were highly hydrophilic since an increase of 13 % in weight, due to adsorbed water, was measured. However, the hydrophobic grafting allowed a significant and progressive decrease of the water adsorption down to only 3 %, as obtained for approximately 1 grafter per nm^2 irrespective of the used precursor. Then, an asymptotic behavior was observed meaning that the extra added precursors had no impact on the silica surface protection against water adsorption.

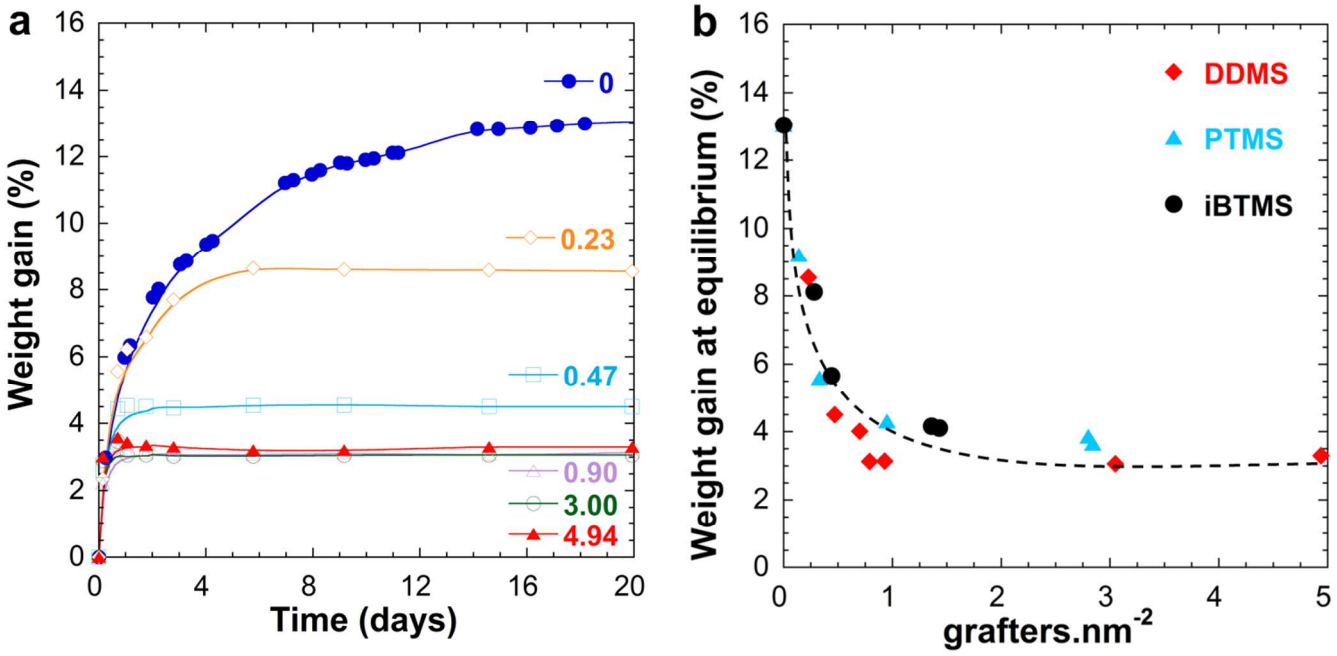

Figure 7. (a) Water uptake kinetics on dried modified silica with dimethoxydimethylsilane at different grafting densities: (●) hydrophilic silica dispersion, (◇) 0.23, (□) 0.47, (△) 0.90, (○) 3.00 and (▲) 4.94 grafters per nm². (b) Weight increase at equilibrium as a function of the grafting density for dimethoxydimethylsilane DDMS (◆), trimethoxy(propyl)silane PTMS (▲) and isobutyl(trimethoxy)silane iBTMS (▼). The dashed line is a guide for the eye. Concerning DDMS, the exact value of the grafters density for the first two points (0.23 and 0.47) is not known due to the detection limit of the TGA method. For these points, values plotted are obtained by interpolation using the known introduced amount and assuming a grafting efficiency of 18 %.

3.6. Discussion. As shown in this work, our original approach which consists in directly hydrophobizing in water silica nanoparticles using organosilanes allowed to precisely control the interactions of the modified silica particles at different stages of concentration and drying, from

dispersed to dried state. Moreover, it also represents an original environmentally friendly route to elaborate, upon simple drying, porous silica materials with damp-proof properties. Indeed, the performed hydrophobization, not only conferred damp-proof properties to the final material, but also had a critical impact on the manner in which silica particles interacted with each other in solution and under drying stress, thus controlling the porosity of the final material.

For low molar grafting ratio, the inter-polymerization of the precursors is limited by the very slow addition of the hydrophobic precursor in the silica dispersion. The probability for two precursors to interact with one another is much lower that the condensation of the hydrolyzed organosilane onto the silica surface. Consequently, the grafting density increases with the introduced ratio on the silica surface until maximum coverage as observed in **Figure 1** whatever the nature of the organosilane's precursor. Above this grafting ratio, the precursor excess will polymerize, forming chains extending away from the silica surface and eventually inducing covalent bonding between silica particles. In that case, the added precursors strongly change the colloidal state of the dispersion (**Figure 2**) and do not participate on the silica surface protection against water adsorption (**Figure 7**). Therefore, it appeared that a value of 1 grafter per nm^2, corresponding to a water adsorption around 3-4 %, was the optimal coverage that can be obtained in those experimental conditions and that above this value, the amount of adsorbed water remained constant. Silica hydrophobization by organosilane precursors was thus never complete since only a fraction of the silanol groups (considering a hypothetical average amount of 5 SiOH per nm^2) could be modified by alkyl chains.[18] The upper limit of the modified surface sites number depends on various steric and kinetics parameters difficult to study independently such as the size of the precursor, the roughness and porosity of the material to modify, the reaction conditions, the number and the nature of the surface silanol groups. The unreacted silanol groups result in a residual hydrophilicity of the surface as observed in the water adsorption experiments, even for high amounts of introduced precursors (water adsorption of 3 % in weight). Nevertheless, this contrasts with a fully hydrophilic surface where water molecules progressively adsorb on the hydroxyl groups and form multilayers (water adsorption of 13 % in weight). To support this discussion, near infrared experiments were

performed at equilibrium (20 days at 25 °C and a relative humidity of 80 %) on both hydrophilic silica particles and silica particles hydrophobized with dimethoxydimethylsilane with a grafting ratio of 3.0. The resulting spectra reported in **Figure 8a** show a set of bands in the region 7500-6500 cm^{-1} characteristics of free silanol groups (7316 cm^{-1}), water molecules hydrogen bonded to silanol group (7121 cm^{-1}) and water molecules bonded with water molecules (6861 cm^{-1}) respectively.[32] In the case of hydrophobized silica particles, the band at 7316 cm^{-1} points the presence of free silanol groups whereas this contribution is nearly inexistent for hydrophilic silica particles. This comparison supports the idea that the grafted hydrophobic organosilanes induce locally a steric hindrance which prevents the water molecules condensation on silanol groups close to the grafter. In addition, water adsorption-desorption isotherms were carried out on both silica and the results are presented in **Figure 8b**. As shown, dried material made from hydrophilic silica particles exhibits a type-IV isotherm presenting a hysteresis loop between a relative pressure range of 0.65 to 0.8, in agreement with a capillary condensation taking place in interstitial pores for a cubic packing (3-6 nm) (**Figure S7** in Supporting Information). This is also supported by the high contribution of water hydrogen bonded water (6861 cm^{-1}) in near infrared experiments (**Figure 8a**). On the other hand, a type-I isotherm is observed in the case of hydrophobized silica which indicates the fact that water molecules mainly adsorb onto silica surface as a monolayer. This observed behavior for hydrophobized silica is consistent with a reported study on porous silica glass grafted with trimethylsilyl groups.[33] In sharp contrast, hydrophilic silica based materials feature a very low porosity with a high water adsorption capacity while hydrophobized materials exhibit a larger residual porosity and only adsorb a low water amount.

Therefore, in the case of hydrophilic silica particles, water molecules form a two-dimensional aqueous network whereas in the case of modified silica water molecules adsorbs on the remaining silanol groups and forms disconnected clusters around the hydrophobic grafters. Based on the water uptake for both hydrophilic and hydrophobized silica (13 and 3 % in weight respectively), the average number of water molecules per silanol groups respectively decreases from 6.2 to 1.8. Both results obtained for hydrophilic and hydrophobized silica are in good agreement with Takei's work which reports (i) a

dramatic increase of the water adsorption obtained at high pressure (multilayers) and (ii) the rupture of the two-dimensional water network in presence of hydrophobic grafters.[33]

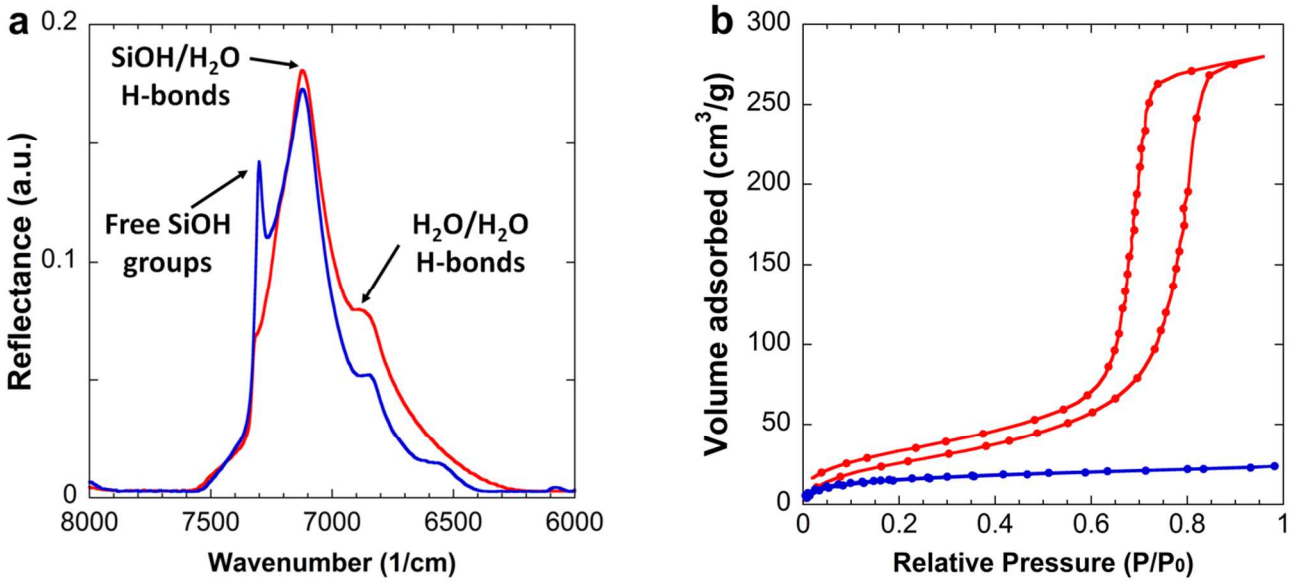

Figure 8. (a) Near infrared spectra at equilibrium and (b) water adsorption-desorption isotherm of pure hydrophilic silica particles (red line) and silica hydrophobized with dimethoxydimethylsilane with a grafting density of 3.0 grafters per nm^2 (blue line). For water adsorption-desorption isotherms, the samples were heated at 100 °C during 15 h under vacuum in order to remove any traces of condensed water.

4. Conclusion

In the present work, we have shown that a controlled hydrophobization of aqueous silica dispersion using organosilane precursors, allowed to finely tune the interparticle interactions and consequently to

change the way the particles assembled under applied drying stress. The resulting nanostructure observed in solution was directly related to the grafting ratio. Indeed, the colloidal state of the modified silica changed from well-dispersed particles for low grafting ratio to small linear chains and finally three-dimensional network for high grafting density. The induced pre-aggregation as well as the interparticle interactions changed upon hydrophobization. This led to the formation of heterogeneous structures during drying resulting in a residual porosity of the fully dried material. Finally, we have demonstrated that the hydrophobization of silica particles with a grafting density of 1 grafter per nm^2 is enough in order to suppress the water condensation onto the silica surface and therefore provides damp-proof properties in the final dried state.

AUTHOR INFORMATION

*E-mail: nicolas.sanson@espci.fr

*E-mail: jean-baptiste.despinose@espci.fr

Notes

The authors declare no competing financial interest.

ACKNOWLEDGMENTS

Electron microscopy was performed at the "Service de Microscopie electronique de l'Institut de Biologie Intégrative IFR 83 (University Pierre and Marie Curie, Paris). The authors thank Dr. G.

Frébourg for the cryo-TEM experiments, Dr. F. Meneau for his help on SWING beamline at ESRF. Water adsorption-desorption isotherms were performed by C. Carteret (Laboratoire de Chimie Physique et Microbiologie pour l'Environnement, Université de Lorraine, Nancy). We thank F. Lequeux for valuable discussions. We gratefully acknowledge Saint-Gobain for financial support.

REFERENCES

(1) Iler, R. K., *The Chemistry of silica*. Wiley: 1979.

(2) Johnsson, A.; Camerani, M. C.; Abbas, Z., Combined Electrospray-SMPS and SR-SAXS Investigation of Colloidal Silica Aggregation. Part I. Influence of Starting Material on Gel Morphology. *Journal of Physical Chemistry B* **2011,** 115, 765-775.

(3) Parneix, C.; Persello, J.; Schweins, R.; Cabane, B., How Do Colloidal Aggregates Yield to Compressive Stress? *Langmuir* **2009,** 25, 4692-4707.

(4) Lafuma, F.; Wong, K.; Cabane, B., Bridging of Colloidal Particles through Adsorbed Polymers. *Journal of Colloid and Interface Science* **1991,** 143, 9-21.

(5) Bauer, D.; Killmann, E.; Jaeger, W., Flocculation and stabilization of colloidal silica by the adsorption of poly-diallyl-dimethyl-ammoniumchloride (PDADMAC) and of copolymers of DADMAC with N-methyl-N-vinyl acetamide (NMVA). *Colloid and Polymer Science* **1998,** 276, 698-708.

(6) Meszaros, R.; Varga, I.; Gilanyi, T., Adsorption of poly(ethyleneimine) on silica surfaces: Effect of pH on the reversibility of adsorption. *Langmuir* **2004,** 20, 5026-5029.

(7) Tavacoli, J. W.; Dowding, P. J.; Routh, A. F., The polymer and salt induced aggregation of silica particles. *Colloids and Surfaces a-Physicochemical and Engineering Aspects* **2007,** 293, 167-174.

(8) Gupta, J. K.; Basu, S., Simultaneous aggregation and sedimentation of silica particles in the presence of surfactants. *Colloids and Surfaces a-Physicochemical and Engineering Aspects* **2005,** 255, 139-143.

(9) Zhou, Z. K.; Wu, P. Q.; Ma, C. M., Hydrophobic interactions and stability of colloidal silica. *Colloids and Surfaces* **1990,** 50, 177-188.

(10) McGovern, M. E.; Kallury, K. M. R.; Thompson, M., Role of solvent on the silanization of glass with octadecyltrichlorosilane. *Langmuir* **1994,** 10, 3607-3614.

(11) Pere, E.; Cardy, H.; Latour, V.; Lacombe, S., Low-temperature reaction of trialkoxysilanes on silica gel: a mild and controlled method for modifying silica surfaces. *Journal of Colloid and Interface Science* **2005,** 281, 410-416.

(12) Takei, T.; Houshito, O.; Yonesaki, Y.; Kumada, N.; Kinomura, N., Porous properties of silylated mesoporous silica and its hydrogen adsorption. *Journal of Solid State Chemistry* **2007,** 180, 1180-1187.

(13) Majors, R. E.; Hopper, M. J., Studies of siloxane phases bonded to silica-gel for use in high-performance liquid-chromatography. *Journal of Chromatographic Science* **1974,** 12, 767-778.

(14) de Monredon-Senani, S.; Bonhomme, C.; Ribot, F.; Babonneau, F., Covalent grafting of organoalkoxysilanes on silica surfaces in water-rich medium as evidenced by Si-29 NMR. *Journal of Sol-Gel Science and Technology* **2009,** 50, 152-157.

(15) Schwertfeger, F.; Frank, D.; Schmidt, M., Hydrophobic waterglass based aerogels without solvent exchange or supercritical drying. *Journal of Non-Crystalline Solids* **1998,** 225, 24-29.

(16) Törncrona, A.; Holmberg, K.; Bordes, R. Modified silica particles. WO 2012/123386 A1. 2012.

(17) Greenwood, P.; Lagnemo, H. Aqueous silica dispersion. WO 2004/035474 A1. 2004.

(18) Zhuravlev, L. T., Concentration of hydroxyl groups on the surface of amorphous silicas. *Langmuir* **1987,** 3, 316-318.

(19) Hayter, J. B., Concentrated colloïdal dispersions viewed as one-component macrofluids. *Faraday Discussions* **1983,** 76, 7-17.

(20) Jullien, R.; Kolb, M., Hierarchical model for chemically limited cluster cluster aggregation. *Journal of Physics a-Mathematical and General* **1984,** 17, L639-L643.

(21) Meakin, P., Reaction limited cluster cluster aggregation in dimensionalities 2-10. *Physical Review A* **1988,** 38, 4799-4814.

(22) Meakin, P.; Muthukumar, M., The effects of attractive an drepulsive interaction on two-dimensional reaction-limited aggregation. *Journal of Chemical Physics* **1989,** 91, 3212-3221.

(23) Babayan, D.; Chassenieux, C.; Lafuma, F.; Ventelon, L.; Hernandez, J., Formation of Rodlike Silica Aggregates Directed by Adsorbed Thermoresponsive Polymer Chains. *Langmuir* **2010,** 26, 2279-2287.

(24) Wong, K.; Lixon, P.; Lafuma, F.; Lindner, P.; Charriol, O. A.; Cabane, B., Intermediate Structures in Equilibrium Flocculation. *Journal of Colloid and Interface Science* **1992,** 153, 55-72.

(25) Cebula, D. J.; Goodwin, J. W.; Jeffrey, G. C.; Ottewill, R. H.; Parentich, A.; Richardson, R. A., Properties of concentrated polystyrene latex dispersions. *Faraday Discussions* **1983,** 76, 37-52.

(26) Matsuoka, H.; Murai, H.; Ise, N., Ordered structure in colloidal silica particle suspensions as studied by small-angle X-ray scattering. *Physical Review B* **1988,** 37, 1368-1375.

(27) Verlet, L., computer experiments on classical fluids .2. Equilibrium correlation functions. *Physical Review* **1968,** 165, 201-214.

(28) Hansen, J. P.; Verlet, L., Phase transitions of Lennard-Jones system. *Physical Review* **1969,** 184, 151-161.

(29) Li, J. Q.; Cabane, B.; Sztucki, M.; Gummel, J.; Goehring, L., Drying Dip-Coated Colloidal Films. *Langmuir* **2012,** 28, 200-208.

(30) Madeline, J. B.; Meireles, M.; Bourgerette, C.; Botet, R.; Schweins, R.; Cabane, B., Restructuring of colloidal cakes during dewatering. *Langmuir* **2007,** 23, 1645-1658.

(31) Ruckdeschel, P.; Kemnitzer, T. W.; Nutz, F. A.; Senker, J.; Retsch, M., Hollow silica sphere colloidal crystals: insights into calcination dependent thermal transport. *Nanoscale* **2015,** 7, 10059-10070.

(32) Christy, A. A., New insights into the surface functionalities and adsorption evolution of water molecules on silica gel surface: A study by second derivative near infrared spectroscopy. *Vibrational Spectroscopy* **2010,** 54, 42-49.

(33) Takei, T.; Yamazaki, A.; Watanabe, T.; Chikazawa, M., Water adsorption properties on porous silica glass surface modified by trimethylsilyl groups. *Journal of Colloid and Interface Science* **1997,** 188, 409-414.

"for Table of Contents use only"

Hydrophobization of Silica Nanoparticles in Water: Nanostructure and Response to Drying Stress

Solenn Moro, Caroline Parneix, Bernard Cabane, Nicolas Sanson,* and Jean-Baptiste d'Espinose de Lacaillerie*